ELSEVIER

Journal of Molecular Catalysis A: Chemical 123 (1997) 163–169

JOURNAL OF MOLECULAR CATALYSIS A: CHEMICAL

Influence of precursors on the sulfated alumina superacid: Support and impregnating solution effect

Tien-syh Yang [a], Tsong-huei Chang [b], Chuin-tih Yeh [a,*]

[a] *Department of Chemistry, Tsing Hua University, Hsinchu 300, Taiwan, ROC*

[b] *Department of Chemical Engineering, Ming-Hsin Institute of Technology and Commerce, Hsinfeng, Hsinchu 304, Taiwan, ROC*

Received 18 November 1996; accepted 3 February 1997

Abstract

Sulfated aluminas (SO_4^{2-}/γ-Al_2O_3) were prepared via impregnation of different commercial γ-Al_2O_3 with different sulfate solutions (H_2SO_4, $Al_2(SO_4)_3$, $(NH_4)_2SO_4$, Na_2SO_4). The amount of superacidic sulfate strongly depended on both precursors of γ-Al_2O_3 and the impregnating solution. A higher loading of superacidic sulfate would be created when γ-Al_2O_3 possessing more strong basic OH groups on the surface was impregnated with stronger acidic solution (H_2SO_4). The amount of the strongly basic OH groups was related to the fraction of octahedral Al^{3+} in the bulk structure. In addition, the $SO_4^{2-}/MgAl_2O_4$ sample was found to have more superacidic sulfate with a stronger acidity ($H_0 \leq -14.5$) than SO_4^{2-}/γ-Al_2O_3 ($H_0 \leq -13.8$) for more and stronger basic OH groups on $MgAl_2O_4$ than γ-Al_2O_3. © 1997 Published by Elsevier Science B.V.

Keywords: Sulfated alumina; Superacid; Derivative thermogravimetry (DTG); Temperature-programmed desorption of ammonia (NH_3-TPD)

1. Introduction

A solid superacid is a solid material which shows an acid strength higher than 100% H_2SO_4 ($H_0 = -12$) [1]. Several types of solid superacids have been developed in literature and applied to acid-catalytic reactions such as isomerization and alkylation of paraffins [2–4], dehydration of alcohols [5,6], etc. The sulfated metal oxides (SO_4^{2-}/MO_x) was one series of solid superacids. Among them, sulfated zirconia (SO_4^{2-}/ZrO_2) with a superacidic strength up to $H_0 \leq -16.0$ and a good activity in *n*-butane isomerization have attracted a great deal of discussion in literature [4,7–11].

Alumina is generally used as the support of industrial catalyst, because it can be formed easily. Arata et al. has reported that sulfated alumina (SO_4^{2-}/Al_2O_3) was a superacid with $H_0 \leq -14.5$ [12] and could be prepared from a well crystallized oxide as γ-Al_2O_3, which has a high surface area and can be obtained commercially. Therefore, the easy forming and preparation of the SO_4^{2-}/Al_2O_3 with a high superacidic density attracted our attention.

In the previous study [13], we have characterized three sulfate species i.e. surface sulfate, multilayer sulfate and crystallized $Al_2(SO_4)_3$ formed in SO_4^{2-}/γ-Al_2O_3 samples. These sulfate species were formed at different concentrations of H_2SO_4 and may be distinguished by the DTG peaks at 950, 630 and 800°C, respectively.

* Corresponding author.

PII S1381-1169(97)00056-3

Among them, only surface sulfate showed a superacidity with $H_0 \leq -13.8$ and was formed at $[H_2SO_4] \leq 0.8$ M. In this article, we intend to understand the effects of precursors (including supports and impregnating solution) on the amount of the superacidic surface sulfate and find the factors to increase this sulfate.

2. Experimental

2.1. Sample preparation

Two series of SO_4^{2-}/γ-Al_2O_3 samples were prepared in this study. One series was prepared by impregnating commercial γ-Al_2O_3 (Merck) with different 0.5 M sulfate containing solution (including H_2SO_4, $Al_2(SO_4)_3$, $(NH_4)_2SO_4$, Na_2SO_4). The other ones were prepared by impregnating different γ-Al_2O_3 (Merck, Kaiser and Degussa, denoted as γ-Al_2O_3(M), γ-Al_2O_3(K), γ-Al_2O_3(D), respectively) with 0.5 M H_2SO_4. $SO_4^{2-}/MgAl_2O_4$ sample was prepared by impregnating $MgAl_2O_4$ (Chinese Petroleum Corp.) with 0.5 M H_2SO_4. All samples were stirred in the impregnating solution for 10 min and then the impregnated slurrys were filtered and dried at 110°C for 12 h and calcined at 550°C for 3 h. Obtained samples were stored in vials as testing samples (sealed with parafilm) for subsequent characterization.

2.2. Thermogravimetric analysis (TGA / DTG)

The content of sulfate in each samples was determined gravimetrically on a Seiko TG/DTA 300 instrument. After a 30 min dehydration at 400°C, the sample temperature was linearly raised (at a rate of 10°C min^{-1}) to 1200°C in an Ar flow (100 ml min^{-1}). Pure γ-Al_2O_3 was used as a blank in the reference port to compensate the possible interference from the desorption of hydroxyl groups on the surface of γ-Al_2O_3. The sulfate loading (SL, wt%) of testing samples was estimated from the weight loss (Δm) between 400 and 1200°C. The SL was further converted into a specific sulfate loading (sSL, with a unit of $N_{SO_4^{2-}}$ nm^{-2}, where $N_{SO_4^{2-}}$ denotes the number of sulfate calculated from the Δm on assuming the evaporated constituent was SO_3). DTG profiles were obtained by differentiating TGA.

2.3. Acidity measurement

The acidic strength of the testing sample was characterized by a Hammett indicator method. The detail procedures may be found from the literature [14]. The indicators used in this article had a pK_a value between -12.4 and -14.5 (Table 3).

The acidic distribution of the testing sample was determined by TPD of ammonia (NH_3-TPD) in a fixed-bed flow reactor. Each sample (0.1 g) was dehydrated by an evacuation at 300°C for 1 h before exposure to a flow of dry NH_3 gas at 100°C. After the sample was saturated with NH_3, excessive and physically adsorbed ammonia were purged away at a similar temperature with an Ar flow (100 ml min^{-1}). The NH_3-TPD was performed from 100 to 600°C in the Ar flow (30 ml min^{-1}). The evolved ammonia was trapped in a boric acid/NH_4Cl solution and titrated by sulfamic acid with a on-line automatic pH titrator.

2.4. FT-IR

The OH vibrational frequency of the testing sample was measured by FT-IR (Nicolet 730) to detect the amphoteric properties of the surface sites. In this study, the disc samples were dehydrated at 300°C for 1 h in a flow system before each measurement.

2.5. ^{27}Al MAS NMR

^{27}Al MAS NMR were measured on a Bruker MSL-300 spectrometer at 78.2 MHz. The spinning rate was about 4 kHz. A $\pi/12$ pulse of 1 μs was used to minimize the electric field gradient (EFG) effects in quantitative work [15]

and the recycle delay was 0.2 s. The chemical shifts were referred to $Al(H_2O)_6^{3+}$ used as an external standard.

3. Result and discussion

Fig. 1 shows the effect of the impregnating solution on the DTG profiles of various SO_4^{2-}/γ-Al_2O_3(M) samples. All DTG profiles displayed a broad band with the maximum intensity around 950°C. The peak comes from the decomposition of the superacidic surface sulfate, as identified in the previous paper [13]. Apparently, the peak area around 950°C (that is SL, sulfate loading estimated from the TG profile) largely depended on the used sulfate solution. Under the same impregnating condition, the samples prepared from H_2SO_4 obtained the largest sulfate loading. On the other hand, the samples from Na_2SO_4 possessed scarce sulfate loading. The sequence of the SL in order of the impregnating solution is $H_2SO_4 > Al_2(SO_4)_3 > (NH_4)_2SO_4 > Na_2SO_4$ (Table 1). Interestingly, the sequence is the same as their acidic strength, characterized by the pH value of the solution (Table 1). This occurrence obviously indicates that the acidity of the impregnating solution plays an important role in the formation of the

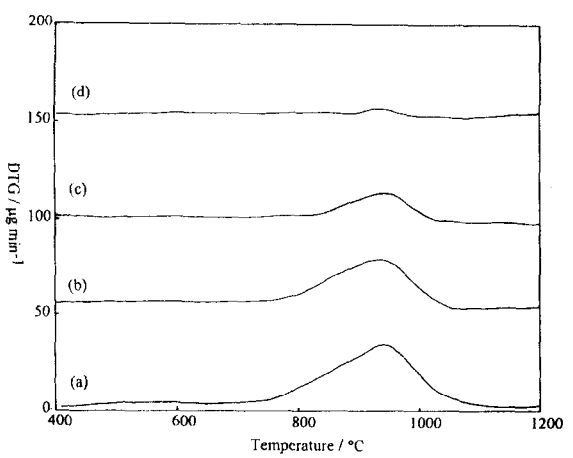

Fig. 1. Effects of sulfate impregnating solution on the DTG profiles of SO_4^{2-}/γ-Al_2O_3(M) samples: (a) H_2SO_4, (b) $Al_2(SO_4)_3$, (c) $(NH_4)_2SO_4$ and (d) Na_2SO_4.

Table 1
pH value of various impregnating solutions and sulfate loadings of corresponding sulfated samples

Samples	pH value of solution [b]	SL (wt%)	sSL ($N_{SO_4^{2-}}$ nm^{-2})
NaS [a]/γ-Al_2O_3(M)	6.07	0.09	0.06
AmS/γ-Al_2O_3(M)	5.32	0.75	0.51
AlS/γ-Al_2O_3(M)	2.51	1.60	1.09
HS/γ-Al_2O_3(M)	0.30	1.88	1.28

[a] NaS, AmS, AlS and HS represent Na_2SO_4, $(NH_4)_2SO_4$, $Al_2(SO_4)_3$ and H_2SO_4, respectively.
[b] $[SO_4^{2-}] = 0.5$ M.

superacidic sulfate. It was proposed that this sulfate was formed in two steps. At first, OH groups on γ-Al_2O_3 were protonated in acidic solution (Eq. (1)) and then, sulfates attacked the Al^{3+} ions easily by removing water (Eq. (2)).

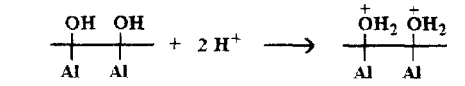

(1)

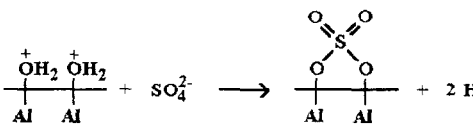

(2)

To understand whether the basicity of OH groups on γ-Al_2O_3 could also influence the formation of the superacidic sulfate, three commercial γ-Al_2O_3 with different amphoteric properties of OH groups were used as the supports to prepare the SO_4^{2-}/γ-Al_2O_3 samples. Fig. 2 displays the segments of IR spectra for three γ-Al_2O_3 supports. These γ-Al_2O_3 showed a quite different vibrational intensity above 3750 cm^{-1}, characterized as basic OH groups by Knozinger et al. [16]. The intensity above 3750 cm^{-1} was in the order of γ-Al_2O_3(K) > γ-Al_2O_3(M) > γ-Al_2O_3(D). Therefore, the IR results indicated that the number of basic OH groups was in the order of γ-Al_2O_3(K) > γ-Al_2O_3(M) > γ-Al_2O_3(D).

Fig. 3 displays the support effect on DTG profiles of sulfated samples. The DTG profiles of three SO_4^{2-}/γ-Al_2O_3 samples showed simi-

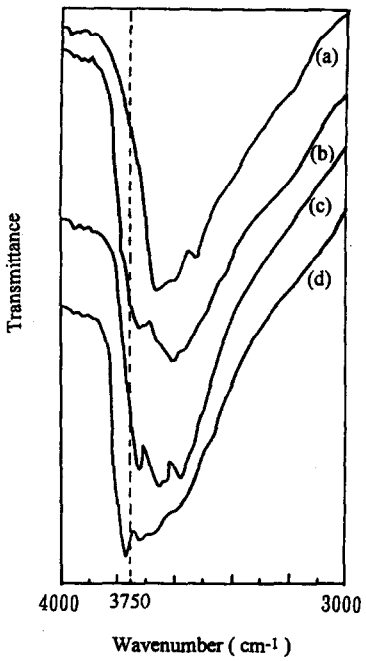

Fig. 2. Segments of FT-IR spectra for three γ-Al_2O_3: (a) γ-Al_2O_3(D), (b) γ-Al_2O_3(K), (c) γ-Al_2O_3(M) and (d) $MgAl_2O_4$.

lar peaks around 950°C but with different peak areas. The peak area (SL) was in the sequence of γ-Al_2O_3(K) > γ-Al_2O_3(M) > γ-Al_2O_3(D) (Table 2). In correspondence with the IR results (Fig. 2), it was demonstrated that more basic OH groups would create more superacidic sulfates.

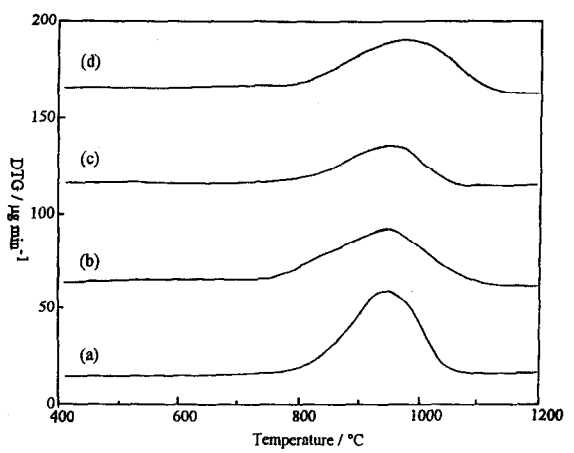

Fig. 3. DTG profiles of three SO_4^{2-}/γ-Al_2O_3 samples: (a) SO_4^{2-}/γ-Al_2O_3(K), (b) SO_4^{2-}/γ-Al_2O_3(M), (c) SO_4^{2-}/γ-Al_2O_3(D) and (d) SO_4^{2-}/$MgAl_2O_4$ sample.

Table 2
Physical properties of various supports and sulfate loadings of corresponding sulfated samples

Samples	Support properties		Sulfate loading	
	area ($m^2 \cdot g^{-1}$)	$F_{oct.}$	SL (wt%)	sSL ($N_{SO_4^{2-}}$ nm^{-2})
SO_4^{2-}/γ-Al_2O_3(D)	118	0.63	1.37	0.87
SO_4^{2-}/γ-Al_2O_3(K)	234	0.69	3.18	1.02
SO_4^{2-}/γ-Al_2O_3(M)	110	0.74	1.88	1.28
SO_4^{2-}/$MgAl_2O_4$	100	0.80	2.15	1.61

According to these results of the impregnating solution effect and the support effect, it was concluded that the formation of the superacidic sulfate was determined by the protonation of the basic OH groups in acidic impregnating solution (Eq. (1)).

The most superacidic sulfate loading of SO_4^{2-}/γ-Al_2O_3(K) sample may be due to the largest surface area of γ-Al_2O_3(K) (Table 2). To exclude the influence of the surface area of γ-Al_2O_3, we compare the specific sulfate loading (sSL and in units of $N_{SO_4^{2-}}$ nm^{-2}, obtained from SL divided by surface area of γ-Al_2O_3) of these samples. The sequential order of sSL became γ-Al_2O_3(M) > γ-Al_2O_3(K) > γ-Al_2O_3(D) (Table 2). Accordingly, it may be suggested that the basic OH groups on γ-Al_2O_3(K) were more than γ-Al_2O_3(M), but those per unit surface area on γ-Al_2O_3(M) were more than γ-Al_2O_3(K).

The number of basic OH groups per unit surface area seem to be difficult to estimate. Knozinger et al. [16] have proposed that the amphoteric properties of OH groups would be influenced by the coordinating condition of Al^{3+} (octahedral or tetrahedral Al^{3+}) linked to OH. From his net charge estimation of OH groups, it may be deduced that more octahedral Al^{3+} in γ-Al_2O_3 would produce more basic OH groups on the surface of γ-Al_2O_3. Hence, we considered that the number of basic OH groups per unit surface area may be predicted by the coordinating condition of Al^{3+} in γ-Al_2O_3. MAS ^{27}Al-NMR is a good technique to detect the ratio of octahedral to tetrahedral Al quantitatively

when using a pulse width smaller $\pi/6$ [15]. Fig. 4 shows the MAS ^{27}Al-NMR of three γ-Al_2O_3. All the samples showed two peaks. One located around 55 ppm was tetrahedral Al^{3+} and the other around 5 ppm was octahedral Al^{3+}. The fraction of octahedral Al^{3+} ($F_{oct.}$) was estimated below.

$$F_{oct.} = I_{oct.}/(I_{tet.} + I_{oct.}) \quad (3)$$

where $I_{tet.}$ and $I_{oct.}$ was the intensity of the corresponding peak in MAS ^{27}Al-NMR spectra. The $F_{oct.}$ result demonstrated the fraction of octahedral Al^{3+} increased in a trend similar to the increasing order of sSL, as shown in Table 2. It is indicated that the number of basic OH groups per unit surface area and subsequently the sSL (loading of the superacidic sulfates per unit surface area) was correlated to the fraction of octahedral Al^{3+}. Hence, γ-Al_2O_3 with a higher surface area and more octahedral Al^{3+} was needed to create a higher density of superacidic sites.

The increase of octahedral Al^{3+} was accompanied with a decrease in the surface area for

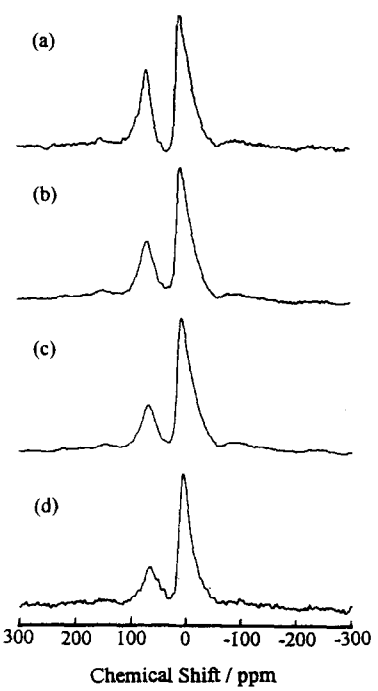

Fig. 4. MAS ^{27}Al-NMR spectras of three γ-Al_2O_3: (a) γ-Al_2O_3(D), (b) γ-Al_2O_3(K), (c) γ-Al_2O_3(M) and (d) $MgAl_2O_4$.

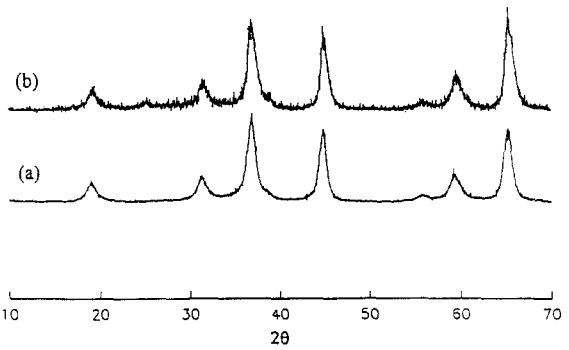

Fig. 5. XRD patterns of (a) $MgAl_2O_4$ and (b) $SO_4^{2-}/MgAl_2O_4$.

the formation of θ- and α-Al_2O_3 as the calcination temperature exceeded 800°C [17]. Therefore, it seems impossible to find a high surface area of γ-Al_2O_3 with all Al^{3+} in octahedral sites. Normal $MgAl_2O_4$ has the structure of a spinel in which all Al^{3+} is in octahedral sites and Mg^{2+} in a tetrahedral position. Therefore, $MgAl_2O_4$ has more and stronger basic OH groups than γ-Al_2O_3, as its IR result shows in Fig. 2. Accordingly, sulfated $MgAl_2O_4$ should have more and stronger superacidity than sulfated γ-Al_2O_3.

Fig. 5 shows the XRD patterns of our used $MgAl_2O_4$ and $SO_4^{2-}/MgAl_2O_4$. The patterns indicated that the $MgAl_2O_4$ had a spinel structure and the structure was not destroyed after sulfation. Fig. 4d shows the MAS ^{27}Al-NMR spectrum of the $MgAl_2O_4$. Its value of $F_{oct.}$ was estimated to be 0.80. The $F_{oct.}$ value indicated that the $MgAl_2O_4$ had some Al^{3+} in tetrahedral sites, but the $F_{oct.}$ was larger than any $F_{oct.}$ of γ-Al_2O_3 used in the present article (Table 2). Hence, the sSL of the $SO_4^{2-}/MgAl_2O_4$ sample was larger than the sSL of SO_4^{2-}/γ-Al_2O_3 samples (Table 2).

The DTG profile of the $SO_4^{2-}/MgAl_2O_4$ sample is shown in Fig. 3d. This sample had a DTG peak around 990°C, which was 40°C higher than the SO_4^{2-}/γ-Al_2O_3 sample. The sulfate in the $SO_4^{2-}/MgAl_2O_4$ sample induced a superacidity at $H_0 \leq -14.5$ (Table 3), also stronger than the SO_4^{2-}/γ-Al_2O_3 samples. The higher thermal stability of the superacidic sulfate may be due to the stronger interaction

Table 3
Acidic strengths of various sulfated samples by a Hammett indicator method

Samples	$H_0 \leq -12.44$ [a]	$H_0 \leq -13.75$	$H_0 \leq -14.52$
$SO_4^{2-}/\gamma\text{-}Al_2O_3$(D)	+ [b]	+	−
$SO_4^{2-}/\gamma\text{-}Al_2O_3$(K)	+	+	±
$SO_4^{2-}/\gamma\text{-}Al_2O_3$(M)	+	+	±
$SO_4^{2-}/MgAl_2O_4$	+	+	+

[a] Indicators used for $H_0 \leq -12.44$ is *p*-nitrofluorobenzene, for $H_0 \leq -13.75$ is 2,4-dinitrotoluene and for $H_0 \leq -14.52$ is 2,4-dinitrofluorobenzene.
[b] '+' shows the color change from the basic form (colorless) to acidic form (yellow) of the indicators, '−' does not, and '±' shows ambiguously.

existing between SO_4^{2-} and OH groups of $MgAl_2O_4$. According to Eqs. (1) and (2), the stronger interaction indicated the basicity of OH groups on $MgAl_2O_4$ was stronger than $\gamma\text{-}Al_2O_3$. Furthermore, the stronger the interaction was, the stronger the inductive effect of SO_4^{2-} on Al^{3+}, therefore, the superacidity of $SO_4^{2-}/MgAl_2O_4$ was stronger than $SO_4^{2-}/\gamma\text{-}Al_2O_3$.

Accordingly, we demonstrated their superacidities by comparing the NH_3-TPD profiles of two $SO_4^{2-}/\gamma\text{-}Al_2O_3$ samples and the $SO_4^{2-}/MgAl_2O_4$ sample. Fig. 6 shows the

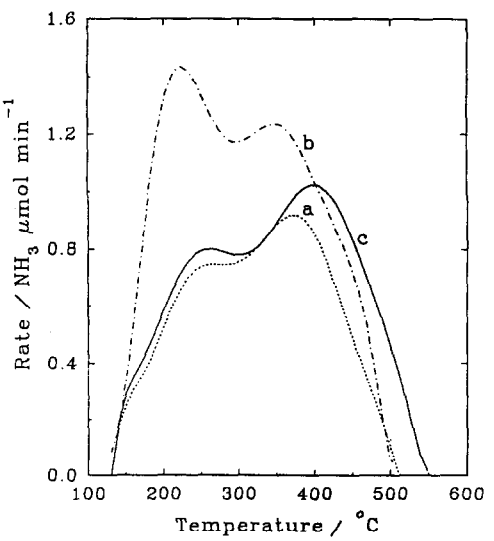

Fig. 6. NH_3-TPD profiles of (a) $SO_4^{2-}/\gamma\text{-}Al_2O_3$(M), (b) $SO_4^{2-}/\gamma\text{-}Al_2O_3$(K) and (c) $SO_4^{2-}/MgAl_2O_4$.

NH_3-TPD profiles of $SO_4^{2-}/\gamma\text{-}Al_2O_3$(M), $SO_4^{2-}/\gamma\text{-}Al_2O_3$(K) and $SO_4^{2-}/MgAl_2O_4$. These samples expressed two peaks in the profiles: a low-temperature peak and a high-temperature peak, corresponding to the weak and strong acid sites, respectively. The NH_3-TPD of $SO_4^{2-}/MgAl_2O_4$ expressed a high-temperature peak around 420°C, while the $SO_4^{2-}/\gamma\text{-}Al_2O_3$ samples showed the peak around 380°C. The result indicated also that the $SO_4^{2-}/MgAl_2O_4$ sample possessed stronger acidic sites than the $SO_4^{2-}/\gamma\text{-}Al_2O_3$ samples.

4. Conclusion

The amount of superacidic sulfate strongly depended on both precursors of $\gamma\text{-}Al_2O_3$ and impregnating solution. The stronger acid strength is the impregnating solution and the more and stronger basic OH groups the supports have, the more superacidic surface sulfates are created. Furthermore, the number of basic OH groups per unit surface area is found to be correlated to the fraction of octahedral Al^{3+}. The $SO_4^{2-}/MgAl_2O_4$ sample possesses larger specific sulfate loading and stronger superacidity than $SO_4^{2-}/\gamma\text{-}Al_2O_3$ samples because $MgAl_2O_4$ has more and stronger basic OH groups per unit surface area than $\gamma\text{-}Al_2O_3$.

Acknowledgements

The authors would like to thank the National Science Council of the Republic of China for financial support through the Contract No. NSC84-2113-M007-018.

References

[1] R.J. Gillespie, T.E. Peel, Adv. Phys. Org. Chem. 9 (1972) 1.
[2] M. Hino, K. Arata, J. Chem. Soc. Chem. Commun. (1979) 1148.
[3] K. Arata, M. Hino, Shokubai 21 (1979) 217.

[4] M. Hino, K. Arata, J. Chem. Soc. Chem. Commun. (1980) 851.
[5] K. Tanabe, A. Kayo, T. Yamaguchi, J. Chem. Soc. Chem. Commun. (1981) 602.
[6] A. Kayo, T. Yamaguchi, K. Tanabe, J. Catal. 83 (1983) 99.
[7] M. Bensitel, O. Saur, J.-C. Lavalley, B.A. Morrow, Mater. Chem. Phys. 19 (1988) 147.
[8] J.C. Yori, J.C. Luy, J.M. Parera, Appl. Catal. 46 (1989) 103.
[9] F. Garin, D. Andriamasinoro, A. Abdulsamad, J. Sommer, J. Catal. 131 (1991) 199.
[10] C. Morterra, G. Cerrato, C. Emanuel, V. Bolis, J. Catal. 142 (1993) 349.
[11] A. Corma, V. Fornes, M.I. Juan-Rajadell, J.M. Lopez Nieto, Appl. Catal. A 116 (1994) 151.
[12] K. Arata, M. Hino, Appl. Catal. 59 (1990) 197.
[13] T.S. Yang, C.T. Yeh, T.H. Chang, J. Mol. Catal. (1996) accepted.
[14] K. Tanabe, M. Misono, Y. Ono, H. Hattori (Eds.), Stud. Surf. Sci. Catal. 51 (1989) 6.
[15] A. Samoson, E. Lippmaa, Phys. Rev. B 28 (1983) 6567.
[16] H. Knozinger, P. Ratnasamy, Catal. Rev. Sci. Eng. 17 (1978) 31.
[17] C.S. John, N.C.M. Alma, G.R. Hays, Appl. Catal. 6 (1983) 341.